MiR-107 inhibits the malignant biological behavior of esophageal squamous cell carcinoma by targeting TPM3

Peipei Zhang[1]^, Weiguang Zhang[1]^, Junfei Jiang[1], Zhimin Shen[1], Sui Chen[1], Shaobin Yu[1], Mingqiang Kang[1,2,3,4]^

[1]Department of Thoracic Surgery, Fujian Medical University Union Hospital, Fuzhou, China; [2]Key Laboratory of Ministry of Education for Gastrointestinal Cancer, Fujian Medical University, Fuzhou, China; [3]Fujian Key Laboratory of Tumor Microbiology, Fujian Medical University, Fuzhou, China; [4]Fujian Key Laboratory of Cardio-Thoracic Surgery, Fujian Medical University, Fuzhou, China

Contributions: (I) Conception and design: P Zhang, W Zhang, M Kang; (II) Administrative support: None; (III) Provision of study materials or patients: None; (IV) Collection and assembly of data: P Zhang, W Zhang, J Jiang; (V) Data analysis and interpretation: P Zhang, S Chen, Z Shen; (VI) Manuscript writing: All authors; (VII) Final approval of manuscript: All authors.

Correspondence to: Mingqiang Kang. Department of Thoracic Surgery, Fujian Medical University Union Hospital, 29 Xinquan Road, Gulou, Fuzhou 350001, China. Email: mingqiang_kang@163.com.

Background: Esophageal squamous cell carcinoma (ESCC) is a highly lethal and aggressive tumor. Our previous study revealed that tropomyosin 3 (TPM3) is up-regulated in the late stage of ESCC and promotes epithelial-mesenchymal transition (EMT) via MMP2/MMP9. However, we have not yet explored the upstream regulator of TPM3. In this study, miR-107, a microRNA molecule, was predicted as an inhibitor targeting TPM3, and *in vivo* and *in vitro* experiments confirmed this hypothesis.

Methods: Western blot and fluorescence quantitative polymerase chain reaction (qPCR) were applied to analyze the expression of miR-107 and TPM3. Flow cytometry, cell counting kit-8 (CCK8) assay, wound-healing assay, colony formation assay, transwell assay, and a BALB/c nude mouse (male, 8 weeks old, 20±2 g) model were used to detect the function of miR-107 and TPM3 in ESCC. Dual-luciferase assay was used to analyze the suppressed TPM3 expression induced by miR-107. Rescue experiments were also conducted in our research.

Results: The cell and nude mouse models verified that TPM3 promotes proliferation, invasion and metastasis, and inhibits apoptosis, which is the opposite effect of miR-107 in ESCC. Meanwhile, the expression of TPM3 was up-regulated in the ESCC sample and cell lines, and miR-107 was down-regulated correspondingly. Dual-luciferase detection confirmed that miR-107 decreased the expression of TPM3 by targeting the 3'-untranslated region (3'-UTR) at the end of the TPM3 transcript. Further experiments verified that TPM3 could rescue the tumor suppression effect derived from miR-107.

Conclusions: MiR-107 negatively regulates TPM3 expression and plays a tumor suppression role in ESCC.

Keywords: Esophageal squamous cell carcinoma (ESCC); miR-107; tropomyosin 3 (TPM3); proliferation; apoptosis

^ ORCID: Peipei Zhang, 0000-0002-3986-9075; Weiguang Zhang, 0000-0002-0191-8054; Mingqiang Kang, 0000-0002-0715-6556.

Introduction

Globally, esophageal cancer (EC) ranks seventh in terms of incidence and sixth in terms of mortality among common malignancies (1). Esophageal squamous cell carcinoma (ESCC), which is the predominant pathological type, accounts for more than 93% of EC patients in China (2). Currently, esophagectomy remains the most reliable treatment measure, and radiotherapy and chemotherapy are also important adjuvant strategies (3,4). However, owing to our lack of understanding of the crucial pathogenesis of ESCC, we have not exploited effective molecular targeted therapeutic drugs (5).

Dysregulation of some crucial proteins may play a negative role in ESCC and other cancers (6,7). The tropomyosin 3 (*TPM3*) gene is located in subband 1, band 3, region 2, long arm of chromosome 1(1q21.3). The TPM3 protein can interact with actin, affecting muscle cell contraction and other cytoskeletal activity (8,9). Meanwhile, *TPM3* gene-related rearrangement has been widely reported in malignant tumors and other diseases, such as colorectal cancer, thyroid cancer, and lung cancer (10-12). Some proteomics-based studies have found that TPM3 expression is abnormal in a variety of cancers and may influence tumor behaviors and therapeutic resistance (13-15).

A non-encoding micro ribonucleic acid (RNA), miR-107 has received widespread attention in recent years, and its abnormal expression level has been reported in numerous cancers (16,17). Some researchers believe that miR-107 plays a cancer-promoting role (17,18), but most studies have shown that miR-107 serves as a cancer suppressor molecule in multiple cancers, including EC, oral squamous cell carcinoma, gastric cancer, and so on (19-21). MiR-107 can combine with the 3'-untranslated region (3'-UTR) of some encoding oncogene transcripts to induce degradation, thereby weakening cancer cell activity, invasion, and drug sensitivity, etc. (22,23).

We have defined 12 up-regulated proteins in ESCC, including TPM3, particularly in late stage ESCC tissues, through two-dimensional gel electrophoresis (2-DE) and mass spectrometry (15). Experiments have revealed that *TPM3* serves as a powerful oncogene both *in vivo* and *in vitro*, and promotes epithelial-mesenchymal transition (EMT) in ESCC cells via MMP2/MMP9 (24). However, the regulatory signals on TPM3 have not yet been explored, which has limited our understanding of tumorigenesis and the development of precision therapy targeting TPM3. We found through bioinformatics analysis that there were several miRNAs may target TPM3, including miR-107 (25,26). Considering the well-defined role of miR-107 in cancers as previously described, we speculate that it may be an efficient upstream signal of TPM3. In this study, we confirmed that miR-107 might inhibit the expression of *TPM3*, thereby mitigating its cancer-promoting effect. We present the following article in accordance with the ARRIVE reporting checklist (available at https://jgo.amegroups.com/article/view/10.21037/jgo-22-575/rc).

Methods

Tissue samples of ESCC patients

ESCC tumor and corresponding adjacent non-cancerous samples were obtained from 15 primary ESCC patients in the Thoracic Surgery Department of Fujian Medical University Union Hospital in 2018. We used the non-cancerous tissue as the control group and ESCC tumor tissue as the experimental group to analyze the expression changes of miR-107 and TPM3. This study was approved by the ethics committee of the Fujian Medical University Union Hospital [No.: 2017 (08)] and was conducted in accordance with the Declaration of Helsinki (as revised in 2013). All patients consented to this study.

Cell lines and cell culture

Human ESCC cell lines, including EC109, KYSE-150, and the non-cancerous esophagus epithelial cell line HEEC, were purchased from the Cellcook Biotech (Guangzhou, China). EC9706, the other ESCC cell line, was obtained from the preservation of the Key Laboratory of the Ministry of Education for Gastrointestinal Cancer (Fuzhou, China). Roswell Park Memorial Institute (RPMI)-1640 (Sigma, USA) was used to culture all of the abovementioned cell lines, with supplementation of 10% (v/v) fetal bovine serum (FBS, NEWZERUM, New Zealand) in a humidified chamber at 37℃.

Plasmids, lentivirus, and transfection

The lentivirus containing the plasmid that carries knockdown sequences for TPM3 was produced by Hanbio (Shanghai, China), which was used to construct stably transfected cell lines. The mature miR-107 mimics, miR-107 inhibitor, and scrambled control were purchased from Anhui General Biosystems (Chuzhou, China). And

Table 1 Sequences of shTPM3 and shNC

Item	Sequence
shTPM3	5'-GATCCGCTCGTAAGTTGGTGATCATTGTTCAAGAGACAATGATCACCAACTTACGAGTTTTTTG-3'
shNC	5'-GATCCGTTCTCCGAACGTGTCACGTAATTCAAGAGATTACGTGACACGTTCGGAGAATTTTTTC-3'

shTPM3, short hairpin ribonucleic acid sequences against TPM3; shNC, the negative control.

Table 2 Primer sequences for qPCR

Gene	Sequence
TPM3	Forward: 5'- AGCAGCATTGTACAGGG-3';
	Reverse: 5'- GTGCAGGGTCCGAGGT-3'
miR-107	Forward: 5'-TGAAAACCGGGCCTTAAAAGAT-3';
	Reverse: 5'- GATCACCAACTTACGAGCCAC-3'
GAPDH	Forward: 5'- GGAGCGAGATCCCTCCAAAAT-3';
	Reverse: 5'- GGCTGTTGTCATACTTCTCATGG-3'
U6	Forward: 5'-CTCGCTTCGGCAGCACA-3';
	Reverse: 5'-AACGCTTCACGAATTTGCGT-3'

qPCR, quantitative polymerase chain reaction.

the transfection was performed using Lipofectamine 2000 (Thermo, USA) according to the manufacturer's instructions. The short hairpin RNA (shRNA) sequences against TPM3 (shTPM3) and the negative control (shNC) are shown in *Table 1*.

Western blot

Cells from the petri dish on ice were scraped and lysed with Radio Immunoprecipitation Assay (RIPA) lysis buffer (with a protease and phosphatase inhibitor). The lysed samples were centrifuged at 12,000 g for 15 minutes at 4 ℃, and thereafter, the supernatant with dissolved protein was separated and taken to the next step. 20% (v/v) loading buffer (Saint-Bio, Shanghai, China), which was then added to each protein extract and boiled together for 10 minutes. The samples were electrophoresed in 12% polyacrylamide gel electrophoresis (SDS-PAGE), and the protein was then transferred to polyvinylidene fluoride membranes (Millipore, USA). Subsequently, the protein bands were incubated with primary antibodies at 4 ℃ for 12 hours and then incubated with secondary antibody at room temperature for 60 min. The following antibodies were used: TPM3 (Proteintech, Wuhan, China), GAPDH (Abcam, Shanghai, China), and secondary antibodies (Bioworld, Nanjing, China).

Fluorescence quantitative polymerase chain reaction (qPCR)

RNA in the cells and tissues was extracted using Trizol reagent (Invitrogen, USA) for both miRNA and messenger RNA (mRNA) analyses. To quantify miRNA, 1 µg total RNA was added to a poly (A) tail by poly (A) polymerase (NEB, Beverly, MA, USA), which was followed by reverse transcription with an oligo (dT) adapter primer. For mRNA quantification, oligo (dT) primers were used to generalize cDNAs from total RNA. The Reverse Transcription Kit (Applied Biosystems, USA) was used to conduct complementary DNA (cDNA) synthesis. The real-time qPCR was processed using the PrimeScript™ RT Master Mix Kit (Takara Bio, Kusatsu, Japan) on an ABI7900 System. GAPDH and U6 were selected as the internal control. The primer sequences are shown in *Table 2*. Each PCR experiment was independently performed at least three times, and the relative expression value was expressed using the $2^{-\Delta\Delta Ct}$ method.

Flow cytometry (FCM)

To measure apoptosis, the cells were initially collected after trypsin digestion and rinsed in an ice bath with phosphate buffered saline (PBS) three times. Subsequently, the cells were resuspended and counted, and each tube contained 1×10^5 cells. Thereafter, the cells were stained with Annexin V and Propidium iodide (PI) (BD Biosciences, USA), of which incubation of 10 min in the dark is necessary for the PI staining. Eventually, the stained cells were analyzed using CytoFLEX (Beckman coulter, USA).

CCK8 assay

Cell Counting Kit-8 (CCK8, Dojindo, Japan) was used to detect the proliferation of ESCC cells. Each group of cells was plated and cultured in 96-well plates with 5×10^3 cells per well for the indicated time. The supernatant was then removed, and the CCK8 solution was added to each well and incubated at 37 ℃ for 1 hour. Finally, the absorbance of

1544

Zhang et al. MiR-107 inhibits TPM3 in ESCC cells

each well at 450 nm was measured by a microplate reader (Molecular Devices, USA). The data analysis was based on the results of three independent experiments.

Colony formation assay

The ESCC cells were seeded and cultured in a 12-well plate (1×10^3/mL) for 1 week. 0.1% crystal violet (Sigma-Aldrich) was used to stain the colonies, and PBS was used to wash each well twice. To evaluate the colony formation ability, the macroscopic violet colonies were counted.

Wound-healing assay

Each group of cells was implanted into a 35-mm plate with 5×10^5 cells per well and scraped using a 20 μL pipette tip when the ESCC cells had grown to 90% confluence. They were then cultured in a serum-free medium, and photos were taken under the microscope at 0 and 24 hours.

Transwell assay

The invasion and migration abilities of cells were detected by a 24-well transwell chamber (Corning, USA). Matrigel coating on the filter membrane determined its specific use in our experiments. The cells were suspended in RPMI-1640 and seeded into the upper chamber with 5×10^4 cells per well, and a complete medium containing 20% FBS was added into the bottom chamber. After 48 hours, crystal violet (0.1%) was used to stain cells for 20 minutes and PBS was used for washing. Image J software (National Institutes of Health, USA) was used to observe and count the cells.

In vivo nude mice model assay

In vivo subcutaneous xenograft tumor model and tail vein injection model were constructed to evaluate the growth and lung metastases of ESCC cells respectively. All animal experiments were approved by the Institutional Animal Care and Use Committee of Fujian Medical University (No.: 2020 Association Ethics Examination No. (040)), in compliance with Chinese National Standard (GBT 35823-2018) Laboratory Animals - General Requirements for Animal Testing. A protocol was prepared before the study without registration. Male BALB/c nude mice (8 weeks, 20±2 g) were selected and purchased from SLAC (Shanghai, China). After a week of adaptation during which no disease occurred, a total of 20 nude mice were prepared

for the next experiments, 10 for each model, 5 each in the experimental group or the control group. Stably transfected cell lines based on EC109 were selected for *in vivo* model. In the subcutaneous xenograft tumor model assay, 1×10^7 ESCC cells transfected with shTPM3 or shNC were resuspended in 100 μL saline medium and then injected into the subcutaneous position of the right forelimbs of both groups. The tumor volume was measured every 5 days, and the nude mice were put to death by cervical dislocation after 30 days. The tumors were subsequently removed, photographed, and weighed. The tumor tissues were taken for paraffin sectioning. Ki-67 immunohistochemistry (IHC) and terminal deoxynucleotidyl transferase nick-end-labeling (TUNEL) staining were applied to evaluate the proliferation and apoptosis of ESCC cells *in vivo*. If the tumor volume reached 2000mm³, the mice were also sacrificed to relieve the pain. In the tail vein injection model assay, ESCC cells transfected with shTPM3 or shNC were prepared as a single cell suspension in saline and injected into the tail veins of the nude mice, with 1×10^6 cells per mice. After 30 days, all of the nude mice were sacrificed, and hematoxylin/eosin (HE) staining was applied to the lung tissue sections. The nude mice were housed in a specific pathogen-free environment (50%±10% relative humidity, 25±1 ℃), and 5 mice per cage. Each operation was performed by the same person to reduce errors, and the mice were treated in the same order. The grouping of mice is known to designers and data analysts, but not to breeders and operators.

Dual-luciferase assay

We predicted that a nucleotide sequence located in the 3'-UTR of the TPM3 transcript might be the binding site of miR-107, which was verified by a dual-luciferase reporter experiment. The mutant sequence of the putative binding site (TPM3-MUT) and the wild-type sequence (TPM3-WT) were respectively cloned downstream of the luciferase reporter gene into the psiCHECK-2 vector. When cells cultured in 12-well plates reached 80% confluence, a 0.5 mg reporter plasmid and 50 nM miR-107 mimics or inhibitors were used to cotransfect cells. After 48 h, luciferase detection was conducted by the Dual-Luciferase Reporter Assay System (Promega, USA). The experiments were carried out three times for each group to be compared.

Statistical analysis

SPSS 22.0 (International Business Machines Corporation,

USA) and GraphPad Prism 8.0 (Dotmatics, USA) were applied to analyze and visualize the data generated in this study. Statistical significance was analyzed using the unpaired Student's t-test or one-way analysis of variance (ANOVA) followed by Bonferroni's multiple as appropriate. Tumor volume, weight and percentage of lung area occupied by metastasis and some other data expressed by as mean values ± standard deviation. P-value less than 0.05 was judged as statistically significant.

Results

Knockdown of TPM3 inhibits the proliferation and induces the apoptosis of ESCC cell lines

We established stable transgenic cell lines that knocked down TPM3 in EC109 and EC9706 to explore the role of TPM3 in ESCC cells. The knockdown group was shTPM3, and shNC, which was transfected with nonsense sequence plasmid, was the negative control group. The blank group did not undergo any treatment. Western blot confirmed that the TPM3 protein level declined markedly in the shTPM3 group, while the shNC group did not change significantly compared with the blank group (*Figure 1A*). CCK8 detection and colony formation assays showed that the proliferation of the shTPM3 group was suppressed compared with other groups *in vitro* (*Figure 1B-1D*). Annexin V/PI double staining and FCM experiments showed that the ESCC cells were more prone to apoptosis when the TPM3 protein level decreased (*Figure 1E*).

TPM3 down-regulation weakens the invasion and migration of ESCC cell lines

The transwell assay showed that fewer cells were penetrating the filter membrane to the outer surface of the bottom of the transwell in the shTPM3 group than that in the shNC and blank groups (*Figure 2A*), regardless of whether the filter membrane was coated with matrigel or not. This indicates that the low expression of *TPM3* inhibits the invasion and migration of ESCC cells. The wound-healing assay also confirmed that the down-regulation of *TPM3* suppressed the migration of cells on both sides of the scratch to the opposite side (*Figure 2B*).

TPM3 promotes ESCC cell proliferation and lung metastasis in vivo

We successfully constructed subcutaneous xenograft models and a lung metastasis model in nude mice, and no mice died spontaneously or were sacrificed before reaching the observation time endpoint. The volume and weight of the xenograft tumor in the shTPM3 group were significantly lower than that in the shNC group in the nude mice experiment (*Figure 3A,3B*). Furthermore, the IHC image showed that lower TPM3 expression was associated with a lower Ki-67 level, and TUNEL detection demonstrated that higher levels of apoptosis were observed in the shTPM3 group (*Figure 3C*). In the tail-vein injection nude mouse model, the percentage of lung area occupied by cancer metastasis of shTPM3 was less than that of shNC (*Figure 3D*).

TPM3 and miR-107 expression in tissues and cell lines

We used the starBase website to predict the upstream key signals (25,26), in which miR-107 may play a crucial role. ESCC tissues and paired adjacent tissues from 15 patients were used to investigate the expressions of miR-107 and *TPM3* by qPCR. *TPM3* was overexpressed in cancer compared with normal tissues, while miR-107 was suppressed in ESCC tissues (*Figure 4A,4B*). EC109, EC9706, KYSE-150, and HEEC were also applied to analyze the relationship between miR-107 and TPM3. The transcription of TPM3 was up-regulated in the ESCC cell lines compared to that in HEEC. In contrast, the level of miR-107 in the ESCC cells was less than that in HEEC (*Figure 4C,4D*). The western blot detection results of TPM3 in cell lines were consistent with the qPCR results (*Figure 4E*).

MiR-107 plays an anti-cancer role in ESCC by inhibiting TPM3 expression

We designed mimics and an inhibitor for miR-107. The miR-107 mimics inhibited the expression of *TPM3* compared with NC mimics, while the miR-107 inhibitor increased the expression level of *TPM3* (*Figure 5A*). The dual-luciferase reporter gene assay confirmed that miR-107 decreased the transcription of TPM3-WT, while the fluorescence intensity did not change significantly in the plasmid containing TPM3-MUT. This confirmed the predicted binding area in 3'UTR (*Figure 5B*), which is a classical kind of regulating pattern between miRNAs and mRNAs (27,28). Furthermore, the experiments revealed that miR-107 mimics limited the proliferation, invasion, and migration, but facilitated the apoptosis of ESCC cell lines. However, these tumor suppression effects could be rescued

1546

Zhang et al. MiR-107 inhibits TPM3 in ESCC cells
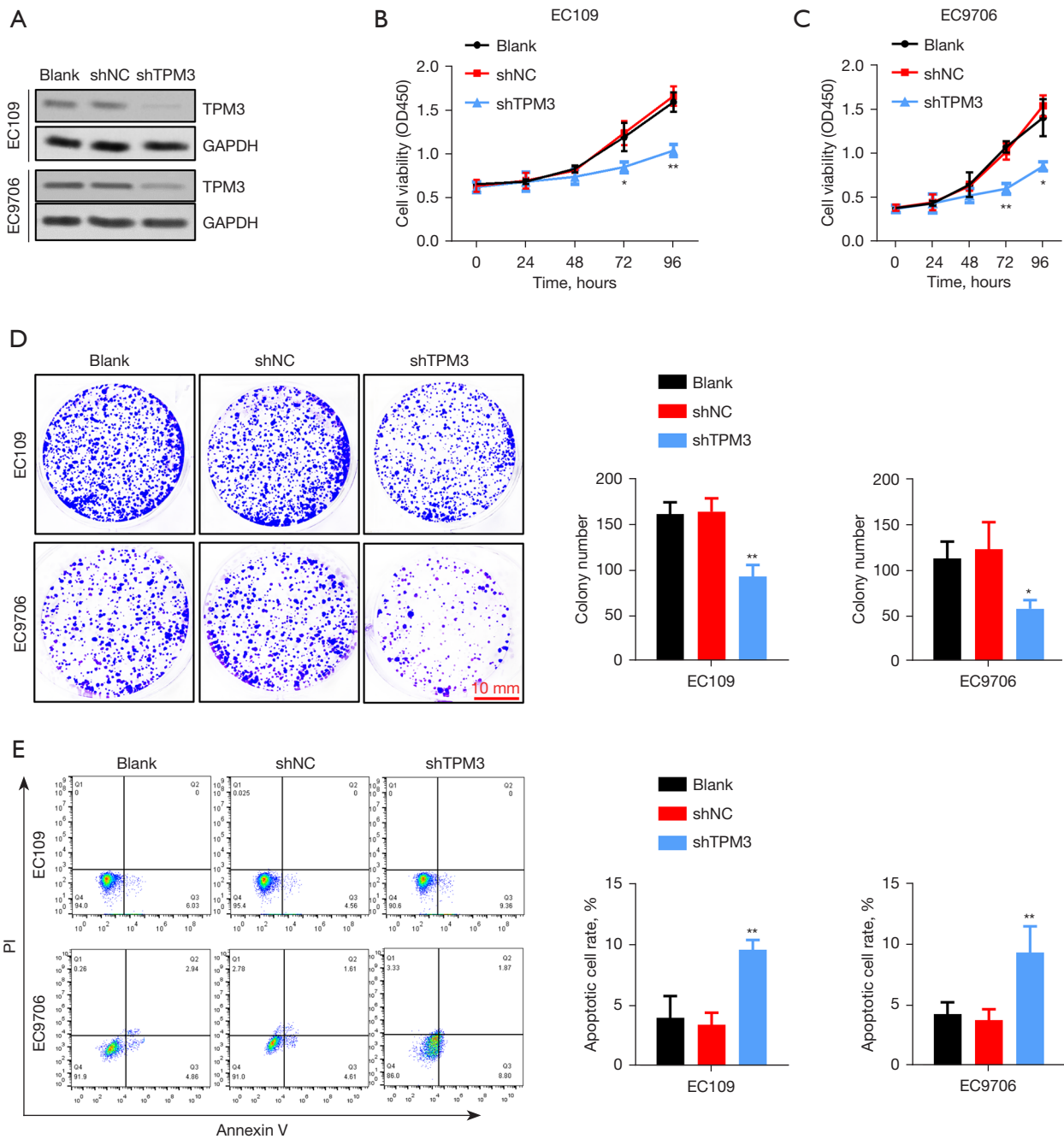
Figure 1 Knockdown of TPM3 inhibits the proliferation and induces the apoptosis of ESCC cell lines. (A) The TPM3 protein expression level was detected by western blot in shTPM3 ESCC cells. (B,C) CCK8 assays detected the proliferation of ESCC cells (n=3). (D) Colony formation assay analyzed the proliferation of ESCC cells, and the number of colonies stained with crystal violet was the basis for comparison (n=3). (E) The proportion of early apoptosis cells in ESCC cells was tested by FCM and Annexin V/PI double staining (n=3). *, ** represent P<0.05, P<0.01 respectively. ESCC, esophageal squamous carcinoma; CCK8, Cell Counting Kit-8; FCM, flow cytometry; PI, propidium iodide.
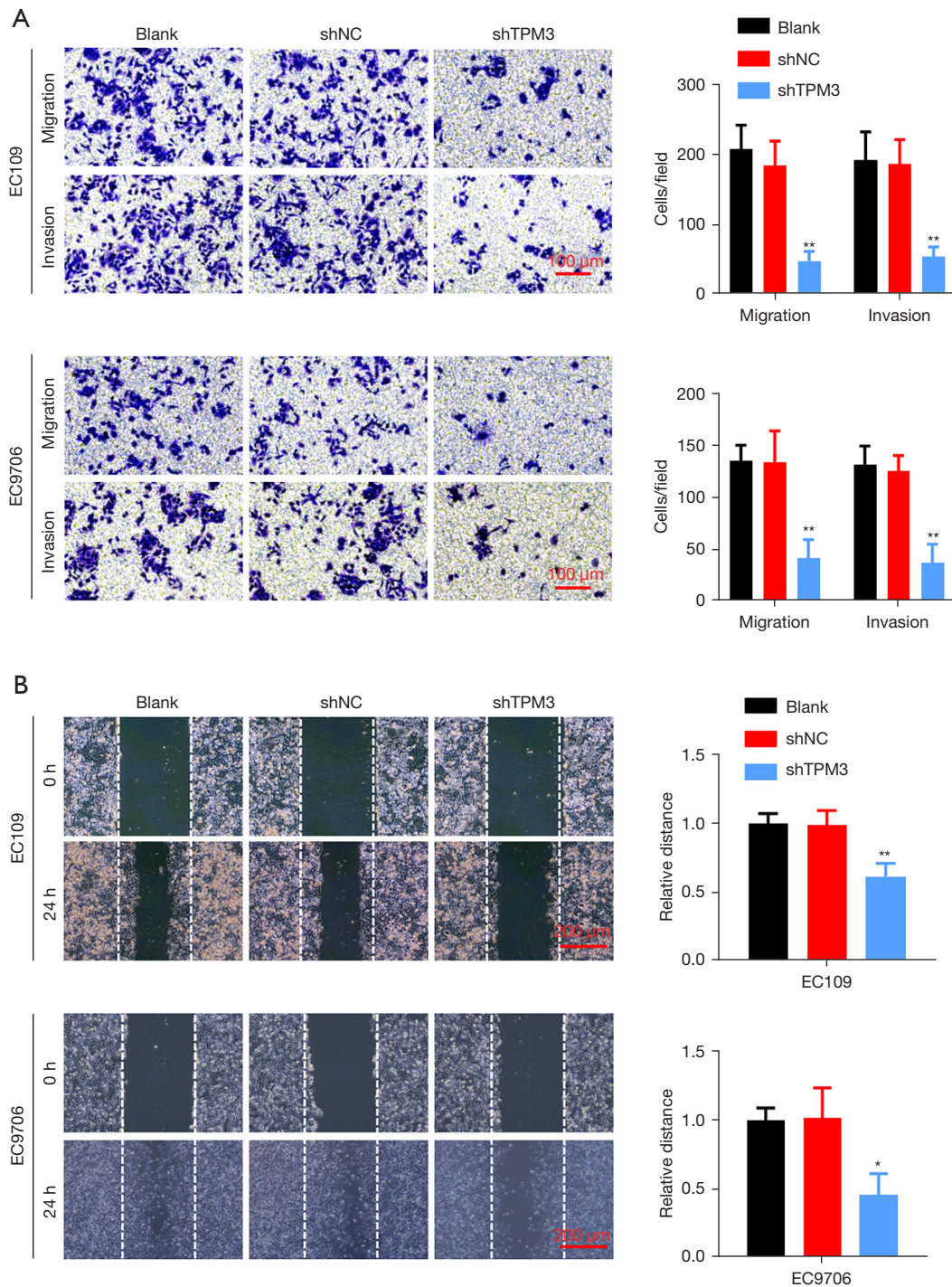
Figure 2 TPM3 down-regulation weakens the invasion and migration of ESCC cell lines. (A) Transwell assays were used to evaluate the invasion and the migration of ESCC cells *in vitro*. The number of cells penetrating the filter membrane coated with matrigel revealed the invasion ability of cells, while the transwell without matrigel could detect the migration of cells (n=3). (B) In the wound-healing assay, the migration of cells was also analyzed, and the distance that cells moved was measured and normalized using the blank group (n=3). All cells were stained with crystal violet. *, ** represent P<0.05, P<0.01, respectively. ESCC, esophageal squamous carcinoma.
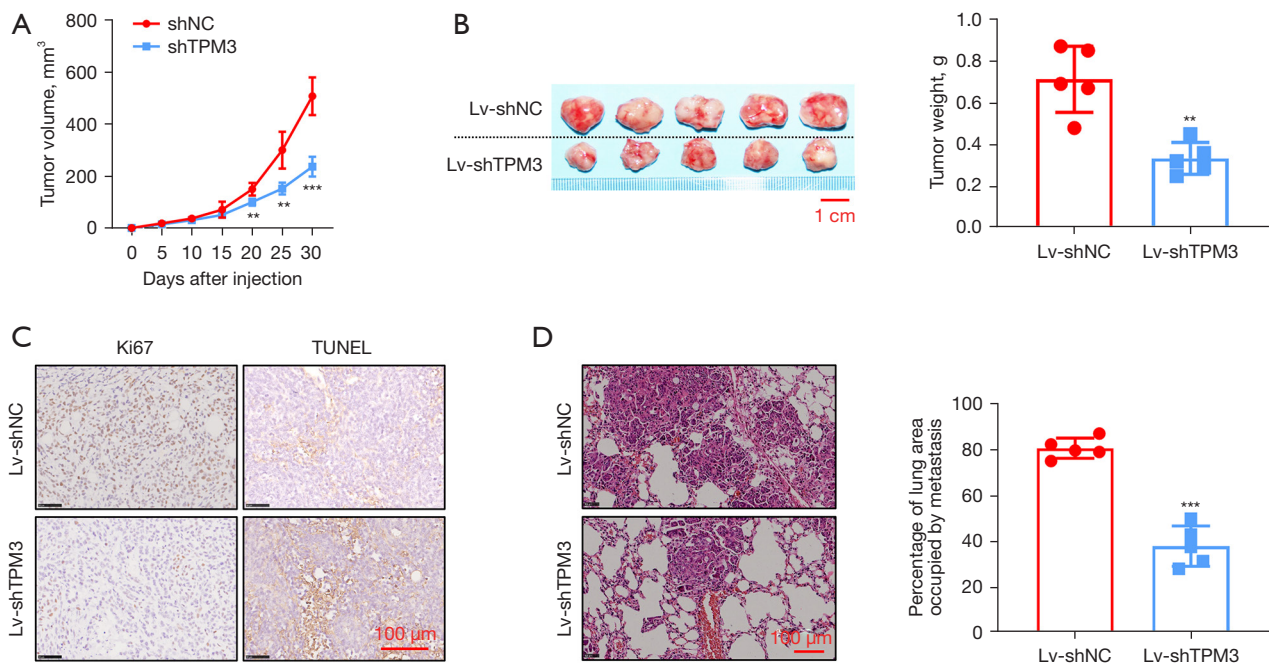
Figure 3 TPM3 promotes ESCC cell proliferation and lung metastasis *in vivo*. (A) The growth curve of subcutaneous tumors in nude mice (day 30, shNC 505.92±72.49 mm³; shTPM3 235.65±38.21 mm³; n=5). (B) Comparison of the size and weight of the removed tumors (day 30, size of tumors: shNC 10.36±0.52 mm, shTPM3 9.14±0.45 mm; weight of tumors: shNC 0.71±0.14 g; shTPM3 0.33±0.07 g; n=5). (C) Detection results of Ki-67 and TUNEL in subcutaneous tumors, and IHC staining were used to detect Ki-67. (D) The tumor percentage in the lungs of the tail-vein injection nude mice metastasis model (day 30, shNC 80.41%±3.95%, shTPM3 37.80%±7.86%; n=5), and the paraffin sections were stained with HE. **, *** represent P<0.01, P<0.001, respectively. ESCC, esophageal squamous carcinoma; TUNEL, terminal deoxynucleotidyl transferase nick-end-labeling; IHC, immunohistochemistry; HE, hematoxylin/eosin.

to some extent by the exogenous plasmid containing *TPM3* (*Figure 6A-6D*).

Discussion

ESCC places a heavy burden on human health. Uncontrolled proliferation, invasion, migration, and resistance to apoptosis are the main characteristics of cancer cells, including ESCC cells (29). Thus, there is a pressing need to explore the molecular mechanisms of malignant biological behaviors of ESCC cells. The present research revealed that miR-107 is suppressed in ESCC tissues and cell lines, while *TPM3* is up-regulated, especially in advanced ESCC tissues (15). *TPM3* is a powerful oncogene that regulates malignant behaviors and the EMT process (24). Our research suggested that miR-107 was a negative regulator of ESCC progression by inducing the degradation of TPM3 mRNA (*Figures 5,6*).

Messenger RNA is a key factor regulating the level of gene expression, and non-coding RNA (ncRNA) often

serves as the regulator of life (30). By interacting with the 3'-UTR of an mRNA, miRNA induces mRNA degradation or prevents mRNA translation (31). Due to only seven to nine nucleotides being complementary between miRNA and its target mRNA, a single miRNA can regulate the expression of multiple genes, eventually reshaping the translated expression profile of a cell system (32). Less commonly, some miRNAs can also promote translation (33). Obviously, miRNAs and mRNAs exhibit an important regulatory relationship that needs to be balanced.

MiR-107 expression is altered in various tumors and is usually regarded as a tumor suppressor regulator (34,35). Down-regulation of miR-107 has been reported in gastric cancer, diffuse large B-cell lymphoma tumors, etc. (19,21,36). The suppression of miR-107 leads to the removal of the functional inhibition of its downstream genes, further promoting the malignant phenotype and resistance to chemotherapy in carcinomas (19,37). High Mobility Group Protein B1 (*HMGB1*), Cyclin-Dependent
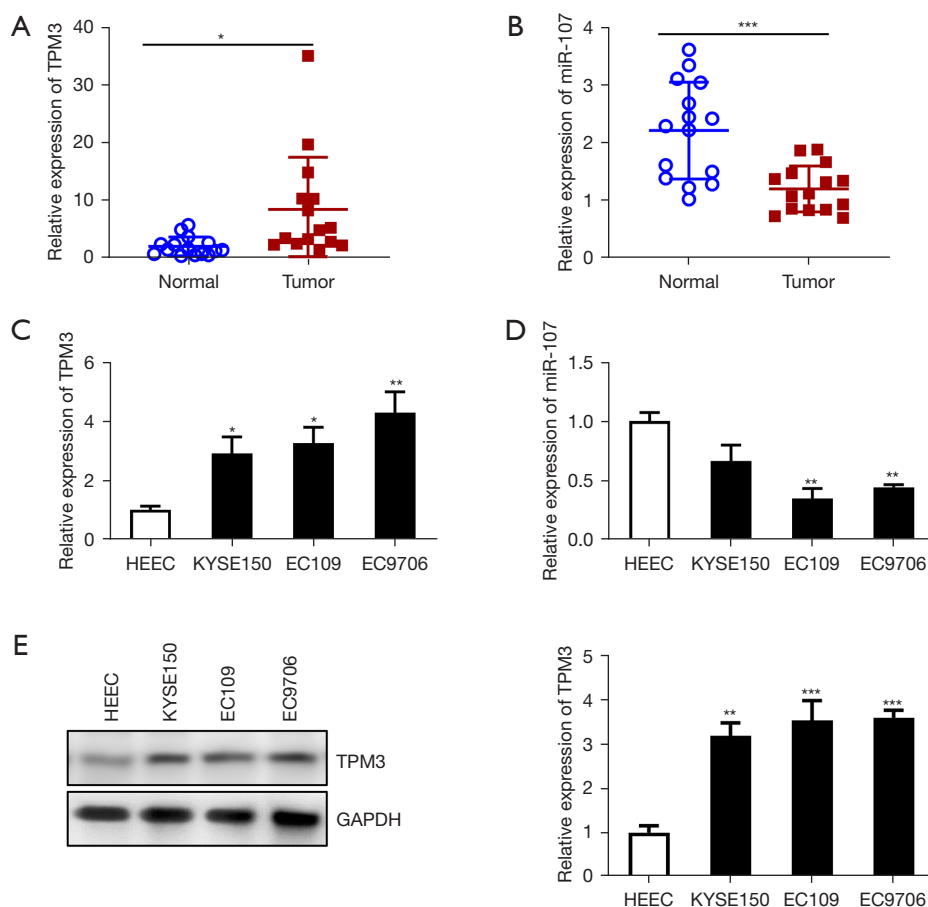
Figure 4 TPM3 and miR-107 expression in tissues and cell lines. (A, B) The qPCR detection results of TPM3 and miR-107 in human ESCC tissues and the paired adjacent normal tissues (n=15). (C, D) The qPCR detection results of TPM3 and miR-107 in human ESCC cell lines and HEEC. (E) The western blot image and the grayscale quantization result. *, **, and *** represent P<0.05, P<0.01, and P<0.001, respectively. qPCR, quantitative polymerase chain reaction; ESCC, esophageal squamous carcinoma; HEEC, human esophageal epithelial cells.

Kinase family (*CDKs*), Brain-Derived Neurotrophic Factor (*BDNF*), Wnt Family Member (*Wnt*), and other famous oncogenes are all negatively regulated by miR-107 (21,33,36-39). On the other hand, some studies have revealed that miR-107 promotes cancer progression by inhibiting Phosphatase and Tensin Homolog Deleted on Chromosome Ten (*PTEN*) expression (40,41).

As for TPM3, considerable research attention has been paid to the fact that *TPM3* can participate in gene fusion and rearrangement, such as *TPM3-NTRKs* (10,11,42), *TPM3-ROS1* (12,43), and so on. Although the proportion is not high, *TPM3* rearrangement is often accompanied by special therapeutic effects (44,45). *TPM3* has also been described as an oncogene, whose encoding product is associated with gastric cancer recurrence (19), breast cancer metastasis (46),

the EMT process of ESCC (24), and liver cancer (47). Our previous studies found that TPM3 up-regulation often indicates an advanced tumor stage in ESCC, and further mechanism analysis has revealed that TPM3 induces EMT in ESCC cells via MMP2/9 activation (15,24).

According to the starBase database (25,26), miR-107 may target TPM3 mRNA. Firstly, we verified that miR-107 facilitates EC109 and EC9706 cell apoptosis, and limits cell proliferation, invasion, and migration. Notably, miR-107 exerts a tumor suppressor role in ESCC, which is the opposite of TMP3. In particular, dual-luciferase reporter analysis revealed that miR-107 is able to directly target TPM3 mRNA and repress TPM3 protein expression in ESCC cells. Further *in vitro* experiments showed that exogenous supplemental TPM3 could rescue the cancer
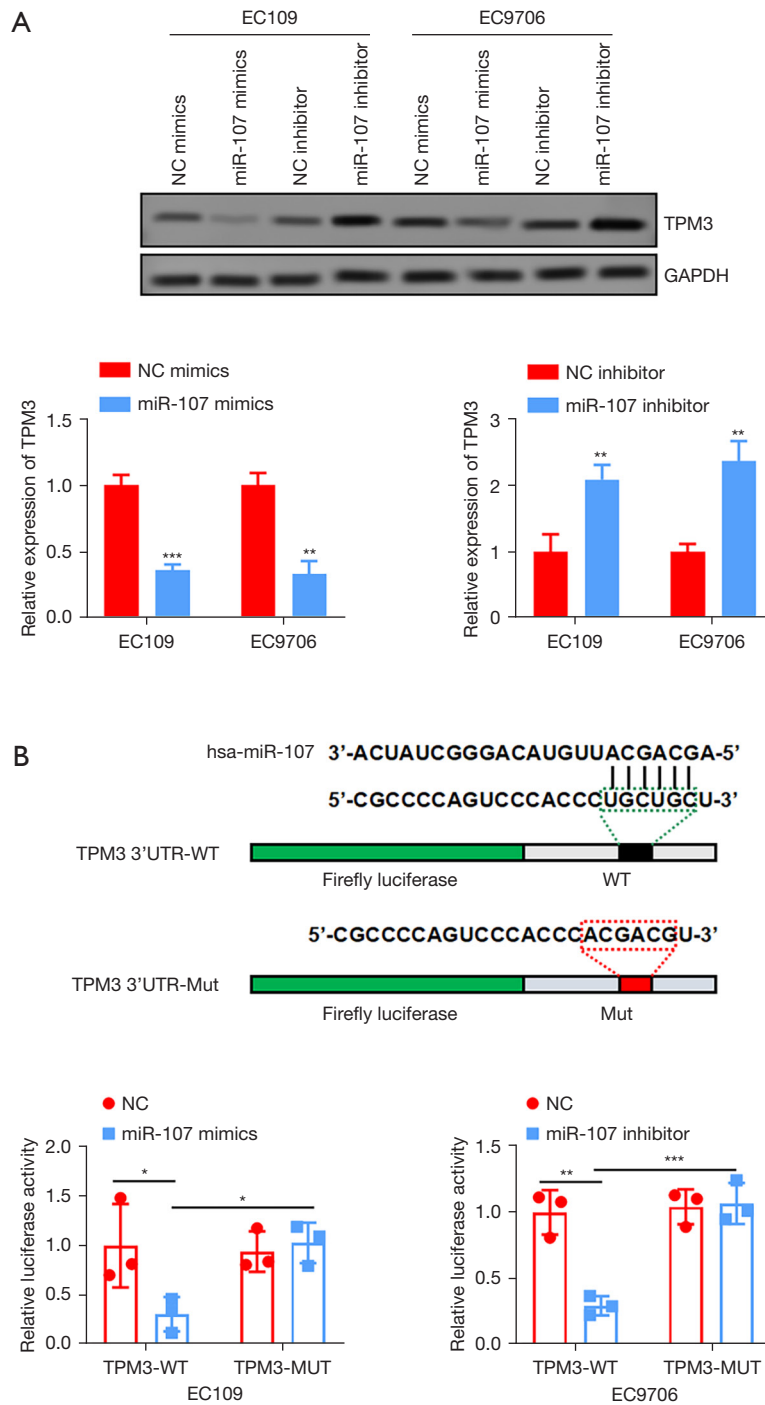
Figure 5 MiR-107 inhibits TPM3 expression by targeting its 3'-UTR. (A) MiR-107 mimics and inhibitor could influence the expression of TPM3, which was confirmed by qPCR and western blot. (B) We designed the mutant sequence (TPM3-MUT) based on the predicted sequence (TPM3-WT) and compared the fluorescence intensity of miR-107 mimics and inhibitor intervention before and after the predicted binding region site mutation in the dual-luciferase reporter gene assay. *, **, and *** represent P<0.05, P<0.01, and P<0.001, respectively. 3'-UTR, 3'-untranslated region; qPCR, quantitative polymerase chain reaction.
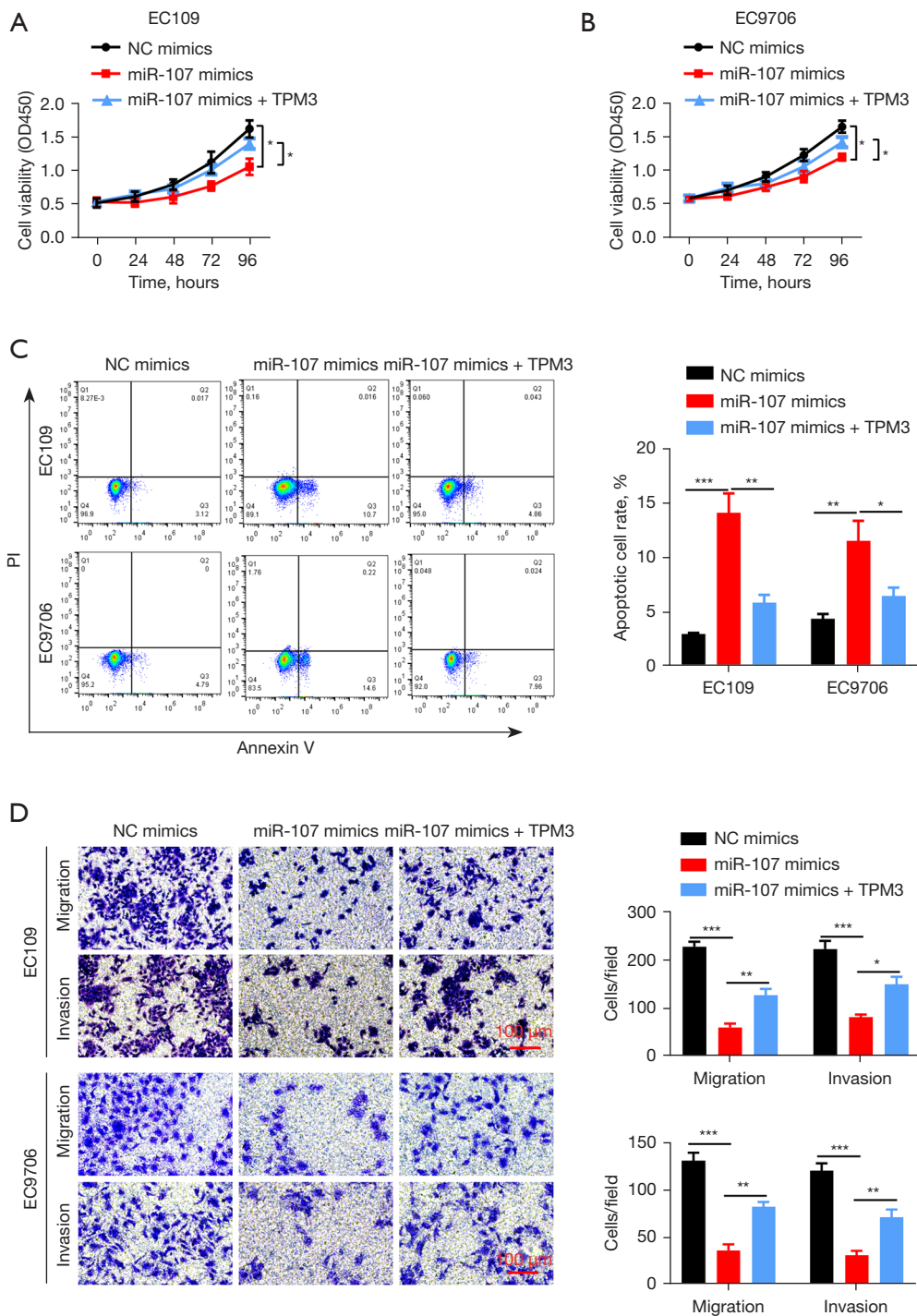
Figure 6 MiR-107 plays an anti-cancer role in ESCC and this effect could be rescued by TPM3. (A,B) Proliferation analysis of ESCC cells based on the CCK8 assay when the miR-107 mimics and exogenous plasmid containing TPM3 were applied (n=3). (C) The detection of early apoptosis levels based on the FCM assay in the case of miR-107 mimics and exogenous TPM3 plasmid intervention (n=3). (D) Transwell experiments results before and after the application of miR-107 mimics and TPM3 plasmid (n=3), here cells were stained with crystal violet. *, **, and *** represent P<0.05, P<0.01, and P<0.001, respectively. ESCC, esophageal squamous carcinoma; CCK8, Cell Counting Kit-8; FCM, flow cytometry.
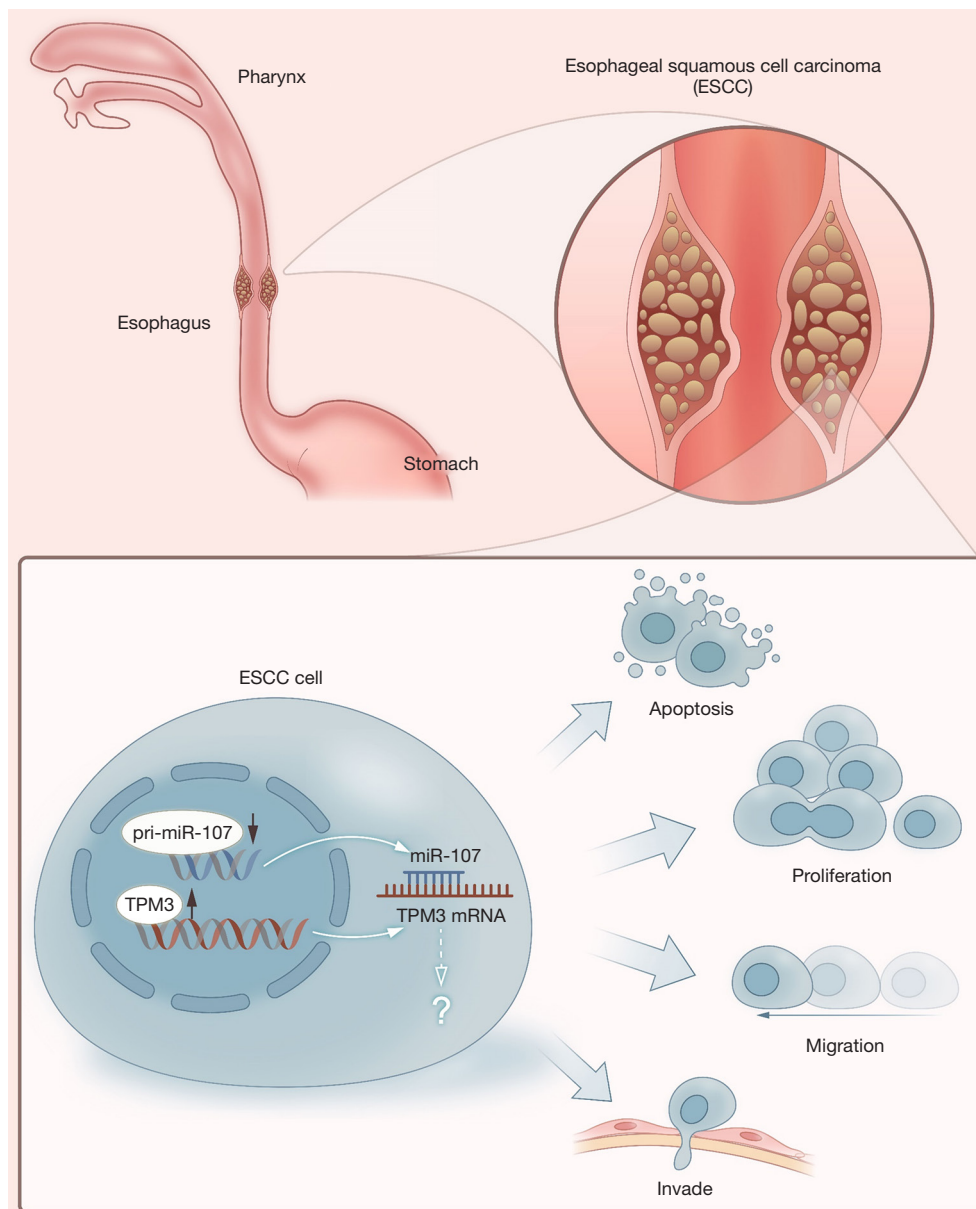
Figure 7 Diagram of miR-107 inhibition of esophageal squamous carcinoma progression by targeting TPM3 expression.

inhibition effect of miR-107. These results confirmed that miR-107 inhibits the ESCC malignant phenotype by negatively regulating TPM3 (*Figure 7*).

Continuing on from our previous research, we identified miR-107 as a negative regulator directly targeting the 3'UTR of the mRNA of TPM3 for the first time. This discovery provides evidence for exploring the mechanism of the tumorigenesis and the advanced process of ESCC and also contributes to the development of cancer treatment strategies. We speculate the changes of miR-107/TPM3 in signal transduction could affect the MMP2/MMP9 expression and activity, further influence the EMT progress of ESCC. But exact molecular mechanisms still need to be discovered and verified by further research. Artificial extracellular vesicles (AEVs) are extremely promising vehicles that can transport molecule keys directionally (48,49). In the present work, miR-107 as a potential effector molecule in ESCC. However, our study could not confirm

the exclusiveness of the regulatory relationship between miR-107 and TPM3, and we did not verify the tumor suppressor effect of miR-107 in animal experiments.

Conclusions

In this study, we focused on the upstream signals of *TPM3*, which had been identified as an oncogene regulating EMT in ESCC (15,24). MiR-107, which exerts a cancer suppression function in ESCC cells, was verified as an inhibitory regulator that directly interacts with the 3'-UTR of TPM3 transcription. Based on this inference, miR-107 may be exploited as an anti-tumor biological effector.

Acknowledgments

Footnote

Reporting Checklist: The authors have completed the ARRIVE reporting checklist. Available at https://jgo.amegroups.com/article/view/10.21037/jgo-22-575/rc

Data Sharing Statement: Available at https://jgo.amegroups.com/article/view/10.21037/jgo-22-575/dss

Conflicts of Interest: All authors have completed the ICMJE uniform disclosure form (available at https://jgo.amegroups.com/article/view/10.21037/jgo-22-575/coif). The authors have no conflicts of interest to declare.

Ethical Statement: The authors are accountable for all aspects of the work in ensuring that questions related to the accuracy or integrity of any part of the work are appropriately investigated and resolved. The study was conducted in accordance with the Declaration of Helsinki (as revised in 2013). The study was approved by the ethics committee of the Fujian Medical University Union Hospital [No.: 2017 (08)]. All patients consented to this study. Animal experiments were performed under a project license (No.: 2020 Association Ethics Examination No. (040)) granted by the Fujian Medical University Institutional Animal Car and Use Committee, in compliance with Chinese National Standard (GBT 35823-2018) Laboratory Animals - General Requirements for Animal Testing.

References

1. Sung H, Ferlay J, Siegel RL, et al. Global Cancer Statistics 2020: GLOBOCAN Estimates of Incidence and Mortality Worldwide for 36 Cancers in 185 Countries. CA Cancer J Clin 2021;71:209-49.
2. Mao YS, Gao SG, Wang Q, et al. Analysis of a registry database for esophageal cancer from high-volume centers in China. Dis Esophagus 2020;33:doz091.
3. Wang H, Tang H, Fang Y, et al. Morbidity and Mortality of Patients Who Underwent Minimally Invasive Esophagectomy After Neoadjuvant Chemoradiotherapy vs Neoadjuvant Chemotherapy for Locally Advanced Esophageal Squamous Cell Carcinoma: A Randomized Clinical Trial. JAMA Surg 2021;156:444-51.
4. Yang W, Liu F, Xu R, et al. Is adjuvant therapy a better option for esophageal squamous cell carcinoma patients treated with esophagectomy? A prognosis prediction model based on multicenter real-world data. Ann Surg 2021. [Epub ahead of print].
5. Yang YM, Hong P, Xu WW, et al. Advances in targeted therapy for esophageal cancer. Signal Transduct Target Ther 2020;5:229.
6. Zheng S, Shen T, Liu Q, et al. CXCL6 fuels the growth and metastases of esophageal squamous cell carcinoma cells both in vitro and in vivo through upregulation of PD-L1 via activation of STAT3 pathway. J Cell Physiol 2021;236:5373-86.
7. Guo X, Zhu R, Luo A, et al. EIF3H promotes aggressiveness of esophageal squamous cell carcinoma by modulating Snail stability. J Exp Clin Cancer Res 2020;39:175.

8. Khaitlina SY. Tropomyosin as a Regulator of Actin Dynamics. Int Rev Cell Mol Biol 2015;318:255-91.

9. Marchenko MA, Nefedova VV, Yampolskaya DS, et al. Comparative structural and functional studies of low molecular weight tropomyosin isoforms, the TPM3 gene products. Arch Biochem Biophys 2021;710:108999.

10. Kim JH, Hong JH, Choi YL, et al. NTRK oncogenic fusions are exclusively associated with the serrated neoplasia pathway in the colorectum and begin to occur in sessile serrated lesions. J Pathol 2021;255:399-411.

11. Pekova B, Sykorova V, Mastnikova K, et al. NTRK Fusion Genes in Thyroid Carcinomas: Clinicopathological Characteristics and Their Impacts on Prognosis. Cancers (Basel) 2021;13:1932.

12. Li W, Guo L, Liu Y, et al. Potential Unreliability of Uncommon ALK, ROS1, and RET Genomic Breakpoints in Predicting the Efficacy of Targeted Therapy in NSCLC. J Thorac Oncol 2021;16:404-18.

13. Yang Z, Yan C, Liu W, et al. Identification of novel autoantibodies in ascites of relapsed paclitaxel-resistant gastric cancer with peritoneal metastasis using immunome protein microarrays and proteomics. Cancer Biomark 2021;31:329-38.

14. Da Costa GG, Gomig TH, Kaviski R, et al. Comparative Proteomics of Tumor and Paired Normal Breast Tissue Highlights Potential Biomarkers in Breast Cancer. Cancer Genomics Proteomics 2015;12:251-61.

15. Yu SB, Gao Q, Lin WW, et al. Proteomic analysis indicates the importance of TPM3 in esophageal squamous cell carcinoma invasion and metastasis. Mol Med Rep 2017;15:1236-42.

16. Du M, Hu X, Jiang X, et al. LncRNA EPB41L4A-AS2 represses Nasopharyngeal Carcinoma Metastasis by binding to YBX1 in the Nucleus and Sponging MiR-107 in the Cytoplasm. Int J Biol Sci 2021;17:1963-78.

17. Li W, Lu H, Wang H, et al. Circular RNA TGFBR2 acts as a ceRNA to suppress nasopharyngeal carcinoma progression by sponging miR-107. Cancer Lett 2021;499:301-13.

18. Liang Y, Zhu D, Hou L, et al. MiR-107 confers chemoresistance to colorectal cancer by targeting calcium-binding protein 39. Br J Cancer 2020;122:705-14.

19. Chang Z, Fu Y, Jia Y, et al. Circ-SFMBT2 drives the malignant phenotypes of esophageal cancer by the miR-107-dependent regulation of SLC1A5. Cancer Cell Int 2021;21:495.

20. Zhu LS, Wang YL, Li R, et al. circ_BICD2 acts as a ceRNA to promote tumor progression and Warburg effect in oral squamous cell carcinoma by sponging miR-107 to enhance HK2. Am J Transl Res 2020;12:3489-500.

21. Wei J, Xu H, Wei W, et al. circHIPK3 Promotes Cell Proliferation and Migration of Gastric Cancer by Sponging miR-107 and Regulating BDNF Expression. Onco Targets Ther 2020;13:1613-24.

22. Gong L, Chen J, Jiang X. Circ_0005033 is an oncogene in laryngeal squamous cell carcinoma and regulates cell progression and Cisplatin sensitivity via miR-107/IGF1R axis. Anticancer Drugs 2022;33:245-56.

23. Peng G, Su J, Xiao S, et al. LINC00152 acts as a potential marker in gliomas and promotes tumor proliferation and invasion through the LINC00152/miR-107/RAB10 axis. J Neurooncol 2021;154:285-99.

24. Chen S, Shen Z, Gao L, et al. TPM3 mediates epithelial-mesenchymal transition in esophageal cancer via MMP2/MMP9. Ann Transl Med 2021;9:1338.

25. Li JH, Liu S, Zhou H, et al. starBase v2.0: decoding miRNA-ceRNA, miRNA-ncRNA and protein-RNA interaction networks from large-scale CLIP-Seq data. Nucleic Acids Res 2014;42:D92-7.

26. Yang JH, Li JH, Shao P, et al. starBase: a database for exploring microRNA-mRNA interaction maps from Argonaute CLIP-Seq and Degradome-Seq data. Nucleic Acids Res 2011;39:D202-9.

27. Xu F, Jiang L, Zhao Q, et al. Whole-transcriptome and proteome analyses identify key differentially expressed mRNAs, miRNAs, lncRNAs and circRNAs associated with HCC. Oncogene 2021;40:4820-31.

28. Shi Z, Wang R, Huang L, et al. Integrative analysis of miRNAs-mRNAs reveals that miR-182 up-regulation contributes to proliferation and invasion of nasopharyngeal carcinoma by targeting PTEN. Aging (Albany NY) 2020;12:11568-78.

29. Hanahan D, Weinberg RA. Hallmarks of cancer: the next generation. Cell 2011;144:646-74.

30. Strobel EJ, Yu AM, Lucks JB. High-throughput determination of RNA structures. Nat Rev Genet 2018;19:615-34.

31. Hoye ML, Regan MR, Jensen LA, et al. Motor neuron-derived microRNAs cause astrocyte dysfunction in amyotrophic lateral sclerosis. Brain 2018;141:2561-75.

32. Lim LP, Lau NC, Garrett-Engele P, et al. Microarray analysis shows that some microRNAs downregulate large numbers of target mRNAs. Nature 2005;433:769-73.

33. Huang V, Place RF, Portnoy V, et al. Upregulation of Cyclin B1 by miRNA and its implications in cancer. Nucleic Acids Res 2012;40:1695-707.

34. Imamura T, Komatsu S, Ichikawa D, et al. Depleted tumor suppressor miR-107 in plasma relates to tumor progression

and is a novel therapeutic target in pancreatic cancer. Sci Rep 2017;7:5708.

35. Ayremlou N, Mozdarani H, Mowla SJ, et al. Increased levels of serum and tissue miR-107 in human gastric cancer: Correlation with tumor hypoxia. Cancer Biomark 2015;15:851-60.

36. Chen X, Xie X, Zhou W. CircCFL1/MiR-107 Axis Targeting HMGB1 Promotes the Malignant Progression of Diffuse Large B-Cell Lymphoma Tumors. Cancer Manag Res 2020;12:9351-62.

37. Chen L, Xu Z, Zhao J, et al. H19/miR-107/HMGB1 axis sensitizes laryngeal squamous cell carcinoma to cisplatin by suppressing autophagy in vitro and in vivo. Cell Biol Int 2021;45:674-85.

38. Zhou Z, Xia N. LncRNA DCST1-AS1 Sponges miR-107 to Upregulate CDK6 in Cervical Squamous Cell Carcinoma. Cancer Manag Res 2020;12:7921-8.

39. Yao J, Yang Z, Yang J, et al. Long non-coding RNA FEZF1-AS1 promotes the proliferation and metastasis of hepatocellular carcinoma via targeting miR-107/Wnt/β-catenin axis. Aging (Albany NY) 2021;13:13726-38.

40. Chen P, Zhao X, Wang H, et al. The Down-Regulation of lncRNA PCAT18 Promotes the Progression of Gastric Cancer via MiR-107/PTEN/PI3K/AKT Signaling Pathway. Onco Targets Ther 2019;12:11017-31.

41. Liu T, Liu S, Xu Y, et al. Circular RNA-ZFR Inhibited Cell Proliferation and Promoted Apoptosis in Gastric Cancer by Sponging miR-130a/miR-107 and Modulating PTEN. Cancer Res Treat 2018;50:1396-417.

42. Yamashiro Y, Kurihara T, Hayashi T, et al. NTRK fusion in Japanese colorectal adenocarcinomas. Sci Rep 2021;11:5635.

43. Cui M, Han Y, Li P, et al. Molecular and clinicopathological characteristics of ROS1-rearranged non-small-cell lung cancers identified by next-generation sequencing. Mol Oncol 2020;14:2787-95.

44. He Y, Sheng W, Hu W, et al. Different Types of ROS1 Fusion Partners Yield Comparable Efficacy to Crizotinib. Oncol Res 2019;27:901-10.

45. Fuse MJ, Okada K, Oh-Hara T, et al. Mechanisms of Resistance to NTRK Inhibitors and Therapeutic Strategies in NTRK1-Rearranged Cancers. Mol Cancer Ther 2017;16:2130-43.

46. Yao B, Qu S, Hu R, et al. Delivery of platelet TPM3 mRNA into breast cancer cells via microvesicles enhances metastasis. FEBS Open Bio 2019;9:2159-69.

47. Choi HS, Yim SH, Xu HD, et al. Tropomyosin3 overexpression and a potential link to epithelial-mesenchymal transition in human hepatocellular carcinoma. BMC Cancer 2010;10:122.

48. Ullah M, Kodam SP, Mu Q, et al. Microbubbles versus Extracellular Vesicles as Therapeutic Cargo for Targeting Drug Delivery. ACS Nano 2021;15:3612-20.

49. Staufer O, Dietrich F, Rimal R, et al. Bottom-up assembly of biomedical relevant fully synthetic extracellular vesicles. Sci Adv 2021;7:eabg6666.

(English Language Editor: A. Kassem)